

Research paper

Mono-copper substituted phosphotungstate supported on to neutral alumina: Synthesis, characterization and detailed studies for oxidation of styrene

Rajesh Sadasivan, Anjali Patel*

Polyoxometalates and Catalysis Laboratory, Department of Chemistry, Faculty of Science, The Maharaja Sayajirao University of Baroda, Vadodra 390002, Gujarat, India



ARTICLE INFO

Keywords:

Copper polyoxometalate
Neutral alumina
Styrene oxidation
Kinetics
Thermodynamics

ABSTRACT

Mono-copper substituted phosphotungstate (PW₁₁Cu) was supported on a neutral support (alumina) by wet impregnation method, which is the first instance of the use of alumina for supporting Transition metal substituted Polyoxometalates (TMSPOMs), characterized by various spectral techniques and the catalytic activity was evaluated for the oxidation of styrene using *tert*-butyl hydroperoxide (TBHP) as oxidant. Various reaction parameters were optimized and a detailed kinetic study was carried out to understand the role of each of the components of the reaction. Finally, the activity of the present catalyst was compared with zirconia supported PW₁₁Cu, and the superiority was explained based on the presence of Lewis acidity of aluminum.

1. Introduction

Polyoxometalates (POMs) are metal oxygen clusters with transition metals in their highest oxidation state (W^{VI}, V^V, Mo^{VI}) and possess the distinct ability to be modified at molecular level. Removal of one or more transition metals gives rise to lacunary POMs (LPOMs) and substitution with other transition metal ions with lower oxidation states, gives rise to transition metal substituted POMs (TMSPOMs). Both LPOMs and TMSPOMs have been widely used as catalysts, however, almost all of them suffer from traditional disadvantages such as high solubility, low surface area, recovery and recycling. To overcome these, various materials have been efficiently used as supports for LPOMs as well as TMSPOMs [1–10]. Supported LPOMs/TMSPOMs possess high thermal, chemical and structural stability [3] and also show advantages over traditional homogeneous catalysts like high surface area, ease of recovery and prevention of corrosion of the reactor.

Amongst, supported TMSPOMs have been of great interest in the last decade, as they provide a two-fold advantage of a lower oxidation state transition metal replacing a high oxidation state one, along with that of a support. Guo et al, in 2009, supported various transition metal substituted polyoxotungstates, K_{10-n}Xⁿ⁺MW₁₁O₃₉ (X = P/Si, M = Co/Ni/Cu/Mn), over modified SBA-15, and used the same for oxidation of styrene [11]. In 2014, Balula et al successfully incorporated zinc-

substituted phosphotungstate over silica nano-sized particles comprising amino-organosilicane surrounded by silica shell, and used the same as catalyst for oxidation of various olefins and also oxidative desulfurization processes [12]. In a different set up in 2015, Romanelli et al synthesized a number of transition metal substituted phosphotungstates using Co, Ni, Cu and Zn, supported them on activated carbon and evaluated the same for the sulfoxidation of 2-(methylthio)-benzothiazole [5]. Patel et al, in 2016, synthesized zirconia supported mono-nickel substituted phosphotungstate, which clearly proved to be a cleaner alternative to traditional techniques for one-pot oxidative esterification of benzaldehyde [13]. Very recently, zinc substituted phosphotungstate was supported on to ionic-liquid modified MCM-41 by Hajian et al and used for selective oxidation of alcohols [2]. Similarly, di-vanadium substituted phosphotungstate was supported over nitrogen-doped carbon nanomaterials by Kholdeeva et al [14] and used for oxidation of various organic substrates.

Numerous reports are available on application of alumina supported POMs as catalysts for various organic transformations [3,10,15]. However, it has never been used to support copper substituted POMs, nor has such a material been used for alkene oxidation. It is well known that supports not only help in providing mechanical hold to the active species, but they also tend to alter the catalytic properties of the material [7]. Hence, recently, as we have reported a detailed study on the flexible

* Corresponding author.

E-mail address: anjali.patel-chem@msubaroda.ac.in (A. Patel).<https://doi.org/10.1016/j.ica.2021.120357>

Received 30 September 2020; Received in revised form 25 February 2021; Accepted 19 March 2021

Available online 23 March 2021

0020-1693/© 2021 Elsevier B.V. All rights reserved.

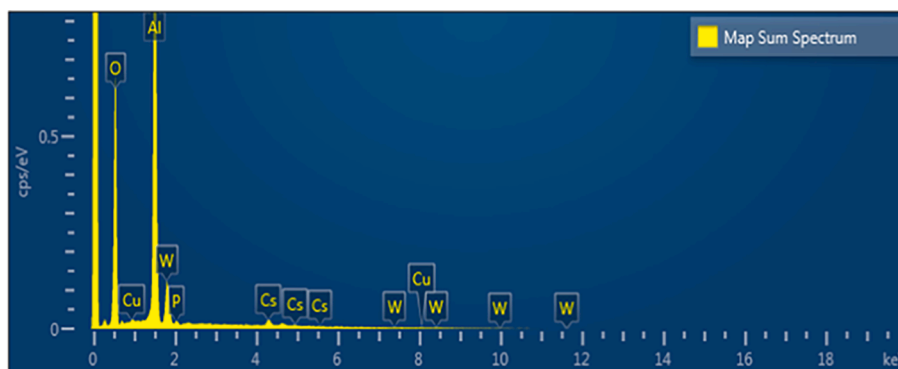


Fig. 1. EDX mapping of $PW_{11}Cu/Al_2O_3$.

oxidation of styrene over mono-copper substituted phosphotungstate ($PW_{11}Cu$) supported on zirconia, it was thought to study the effect of different supports on the activity of $PW_{11}Cu$. It is well known that heteropoly compounds cannot be supported over basic supports, as this may lead to decomposition of the same, we have selected neutral Al_2O_3 as a support for $PW_{11}Cu$, thereby synthesizing a novel heterogeneous catalyst for alkene oxidation. The synthesized material was characterized using various physico-chemical techniques and investigated for the oxidation of styrene using THBP as oxidant, because of the industrial importance of benzaldehyde as well as styrene oxide. Studies for regeneration and recycling were also carried out and a detailed kinetic study was also carried out to understand the role of each component of the reaction. Finally, thermodynamic parameters were determined in order to understand the effect of nature of support.

2. Experimental

2.1. Materials

All chemicals used were of A.R. grade. 12-tungstophosphoric acid, Copper chloride dihydrate, Cesium chloride, styrene, dichloromethane, 70% *tert*-butyl hydroperoxide and neutral aluminium oxide (γ -Alumina) were obtained from Merck and were used as received.

2.2. Synthesis of undecatungstophospho(aqua) cuprate(II) [16]

10 mL solution of 12-tungstophosphoric acid (PW_{12}) (2.88 g; 1 mmol) was adjusted to 4.8 pH using supersaturated NaOH solution (~5 g in 20 mL water) and heated to 90 °C with stirring. To this POM solution, $CuCl_2 \cdot 2H_2O$ (0.17 g; 1 mmol) dissolved in 5 mL water was added drop-wise followed by air-refluxing for 1.5 h at 90 °C. This solution was then filtered hot and solid CsCl (0.5 g) was immediately added. The resulting greenish blue precipitates were filtered, dried at room temperature and designated as $PW_{11}Cu$.

2.3. Supporting of $PW_{11}Cu$ on to neutral alumina.

$PW_{11}Cu$ was supported on to neutral alumina by wet impregnation method. 1 g γ - Al_2O_3 was added to aqueous solution of $PW_{11}Cu$ (0.3 g/30 mL) and left to age for 35 h at room temperature with continuous stirring. This mixture was then dried at 100 °C for 10 h and the resultant material was designated 30% $PW_{11}Cu/Al_2O_3$. On similar lines, 10%, 20% and 40% $PW_{11}Cu/Al_2O_3$ were prepared and as designated.

2.4. Acidity determination by *n*-butylamine titration

Total acidity of the material was determined by technique reported in literature [17]. 0.25 g of material was suspended in a 0.025 M solution of *n*-butylamine in toluene for 24 h. The excess base was titrated

against trichloroacetic acid using neutral red indicator.

2.5. Acid sites determination by potentiometry

The different types of acidic sites were determined by potentiometric titrations using *n*-butylamine [18]. 0.25 g of the synthesized material was suspended in 50 mL acetonitrile and aged at 25 °C. To this, 0.1 mL of 0.05 N *n*-butylamine in acetonitrile was added at regular time intervals and the potential (mV) after each addition was recorded.

2.6. Characterization

The synthesized material was characterized for its acidic strength, and also by thermo gravimetric-differential thermal analysis (TG-DTA), EDX, Brauner-Emmett-Teller (BET) surface area analysis, Temperature Programmed Reduction (TPR), Fourier Transform-Infrared (FT-IR) spectroscopy, FT-Raman spectroscopy, ^{31}P Magic Angle Spin Nuclear Magnetic Resonance (MAS NMR) Spectroscopy and Powder X-Ray Diffractometry (XRD). Elemental analysis of the solid catalyst was carried out by Hitachi Regulus8100. Adsorption-desorption analysis for specific surface area calculations was carried out in the Micrometrics ASAP 2010 instrument at -196 °C. TGA was carried out using Mettler Toledo Star SW 7.01 instrument up to 550 °C. The TPR studies were investigated in a self-made reactor set-up with a quartz reactor vessel. 50 mg of sample was taken and heated up to 800 °C and the linear ramping rate was 10 °Cmin⁻¹ with 5% (35 mLmin⁻¹) H_2/Ar flow for 60 min. the consumption of H_2 gas was monitored using GC instrument equipped with TCD (m/s, CIC Instruments, India). FT-IR spectra of the sample were obtained by using the KBr pellet on the Perkin Elmer instrument. ^{31}P MAS NMR was recorded in JOEL ECX 400 MHz High Resolution Multinuclear FT-NMR spectrometer for solids. Powder XRD analysis was carried out in a Phillips PW-1830 instrument (Cu K α source; scanning range 5^o to 80^o)

2.7. Catalytic reaction

Oxidation of styrene was carried out using $PW_{11}Cu/Al_2O_3$ as catalyst, in a 50 mL batch reactor attached to a double-walled air condenser on a magnetic stirrer and heating plate. 1 mL (10 mmol) of styrene was taken, to which adequate quantities of the catalyst and TBHP were added. Dichloromethane was used to extract the products after the reaction, which were then analyzed in Shimadzu-2014 Gas Chromatograph, using an RTX-5 capillary column. The products were identified by comparison with authentic samples.

Conversion and selectivity of each product was calculated as follows:

$$\text{Conversion} = \frac{(\text{initialmol}\%) - (\text{finalmol}\%)}{(\text{initialmol}\%)} \times 100$$

Table 1
n-Butyl amine acidity values.

Material	Acidity (mmol <i>n</i> -butyl amine/g)
Al ₂ O ₃	0.2
PW ₁₁ Cu	0.5
10% PW ₁₁ Cu/Al ₂ O ₃	0.43
20% PW ₁₁ Cu/Al ₂ O ₃	0.61
30% PW ₁₁ Cu/Al ₂ O ₃	0.83
40% PW ₁₁ Cu/Al ₂ O ₃	0.72

Table 2
Acidic strength and acidic sites determined by potentiometry.

Material	Acidic strength (mV)	Types of acidic sites			Total no. of acidic sites
		Very strong	Strong	Weak	
Al ₂ O ₃	-30	0	0	0.1	0.1
PW ₁₁ Cu	20	0	0.1	0.3	0.4
10% PW ₁₁ Cu/Al ₂ O ₃	62	0	0.1	0.4	0.5
20% PW ₁₁ Cu/Al ₂ O ₃	88	0	0.1	0.9	1.0
30% PW ₁₁ Cu/Al ₂ O ₃	113	0.1	0.1	1.3	1.5
40% PW ₁₁ Cu/Al ₂ O ₃	83	0	0.1	1.7	1.8

$$\text{Selectivity} = \frac{\text{moles of product formed}}{\text{moles of substrate consumed}} \times 100$$

Further, Turn Over Number (TON) was calculated using the equation:

$$\text{TON} = \frac{\text{moles of product}}{\text{moles of catalyst}}$$

2.8. Leaching test

Polyoxometalates can be easily characterized by a clear heteropoly blue colour when reacted with a mild reducing agent like ascorbic acid. This method was used to check for leaching of PW₁₁Cu from the support [19].

3. Results and discussion

3.1. Catalyst characterization

The EDX mapping of PW₁₁Cu/Al₂O₃ (Fig. 1) shows the presence of all elements. The ascertained EDX values (% wt): P, 0.21; W, 13.96; Cu, 0.39; Cs; 4.64 are in good agreement with the theoretical calculated value (% wt): P, 0.20; W, 13.36; Cu, 0.41; Cs; 4.38.

Initially the catalyst was subjected to treatment with ascorbic acid solution. 1 g of the catalyst was refluxed for 24 h in 10 mL distilled water, after which, 10% ascorbic acid solution was added. Absence of blue colour under warm conditions indicated that leaching of PW₁₁Cu does not take place from the support. This also shows existence of strong interactions between the active species and support. Further, the total acidity of the synthesized materials was determined by *n*-butyl amine titrations and the results are presented in table 1. It can be noted that the acidity of the material increases with increase in %loading. This may be attributed to two reasons. The acidity of unsupported PW₁₁Cu itself is very less, and with increase in loading on alumina there is steady increase in overall acidity of the material, which is as expected. Decrease in acidity value from 30% to 40% loading may be due to blocking of acidic sites as a result of higher loading.

The various acidic sites were calculated by potentiometric titration method and the acidic strength in terms of initial electrode potential as

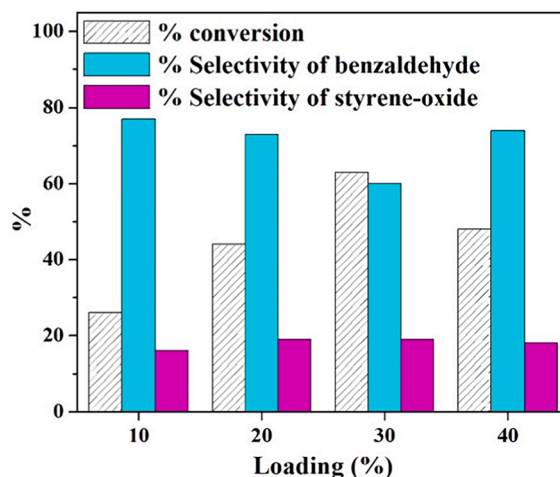


Fig. 2. Effect of % loading (Catalyst amount – 25 mg; Time – 16 h; TBHP – 2 mL; Temperature – 60 °C).

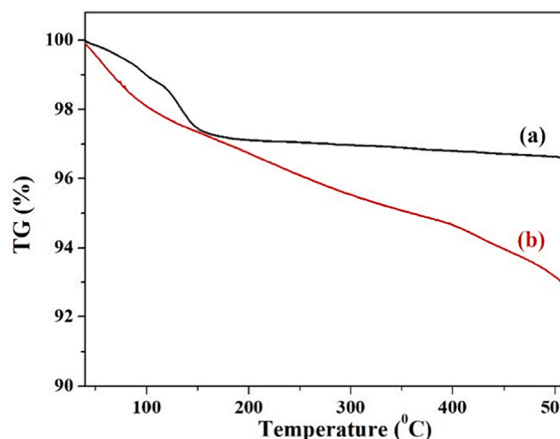


Fig. 3. TGA of (a) PW₁₁Cu and (b) PW₁₁Cu/Al₂O₃.

well as total number of acidic sites are presented in table 2. Neutral alumina shows no significant acidic strength as well as acidic sites. Similarly, the acidic strength of PW₁₁Cu is also very small. Supporting increases the acidity as well as acidic strength of the catalyst to a great extent and as it can be seen from table 2, increase in % loading shows corresponding rise in strength as well as acidic sites. However, the acidic strength for 40% loaded catalyst is significantly lesser than that of 30% loaded one, despite its higher acidic sites. This is attributed to blocking of catalytic sites and is in good agreement with the results obtained from *n*-butylamine titration. Thus, from the acidity determination by *n*-butylamine titration as well as by potentiometry, 30% loading was found to be optimum for carrying out detail characterization.

In order to confirm the same, preliminary reaction was carried out for the oxidation of styrene varying the % loading of PW₁₁Cu (Fig. 2). A steady increase in conversion along with high selectivity for benzaldehyde is seen from 10% to 30% loading which is expected because of the increasing acidity of the catalyst. With further increase in loading there is drastic decrease in the conversion, attributed to blocking of catalytic sites and also confirming the observations of acidity experiments. Hence, 30% loading was considered optimum and further characterization and catalytic activity were done with 30% PW₁₁Cu/Al₂O₃, designated as PW₁₁Cu/Al₂O₃.

TGA of PW₁₁Cu and PW₁₁Cu/Al₂O₃ are shown in fig. 3. The TGA of PW₁₁Cu/Al₂O₃ shows an initial weight loss of 2.1% up to 150 °C attributed to loss of adsorbed water molecules. Further, weight loss of

Table 3

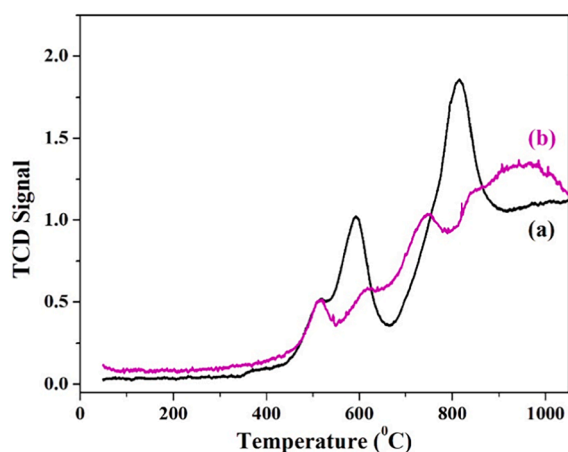
FT - IR frequencies.

FT-IR Frequencies (cm ⁻¹)	P—O	W=O	W—O—W	Cu—O	O—H	H—O—H	O—H—O
Al ₂ O ₃	—	—	—	—	3365	1625	1396
PW ₁₁ Cu/Al ₂ O ₃	1099 1064	—	—	—	3437	1627	—
PW ₁₁ Cu	1103 1061	964	887 810	489	—	—	—

Table 4

FT - Raman frequencies.

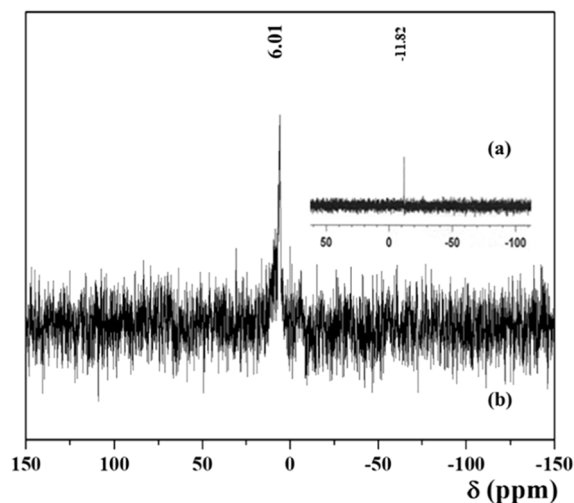
Raman Frequencies (cm ⁻¹)	W=O	W—O	W—O—W	Cu—O
PW ₁₁ Cu	996	985 215	967 946	483
PW ₁₁ Cu/Al ₂ O ₃	1004	980 232	972	485

**Fig. 4.** H₂-TPR curve of (a) PW₁₁Cu and (b) PW₁₁Cu/Al₂O₃.

5.3% between 180 and 500 °C may be due to loss of crystallization water molecules, as well as condensation of surface hydroxyl groups of alumina, which is generally observed in all metal oxide supports. The higher temperature recorded for the loss of adsorbed water in supported catalyst compared to unsupported one, is attributed to strong chemical interactions between the PW₁₁Cu and support. This indicates that the stability of the material is further enhanced on supporting.

The FT-IR frequencies of Al₂O₃, PW₁₁Cu/Al₂O₃ and PW₁₁Cu are given in table 3 and their spectra are presented in figure S1. Alumina shows characteristic bands at 3365, 1625 and 1396 cm⁻¹ corresponding to O—H, H—O—H and O—H—O stretching vibrations respectively. Further, broad bands between 1000 and 400 cm⁻¹ correspond to the various Al—O vibrations. Band around 900 cm⁻¹ corresponds to Al—O stretching vibrations while a band at 763 cm⁻¹ corresponds to Al—O stretching vibrations and the peaks between 700 and 500 cm⁻¹ are assigned to AlO₆ vibrations [20,21]. PW₁₁Cu shows characteristic bands at 1103 and 1061, 964, 887 and 810 cm⁻¹ corresponding to P—O, W=O and W—O—W stretching vibrations respectively. Also, the band obtained at 489 cm⁻¹ corresponds to Cu—O frequency [16]. PW₁₁Cu/Al₂O₃ shows bands at 1099 and 1064 cm⁻¹ corresponding to P—O stretching vibrations of PW₁₁Cu. Apart from this, bands at 3437 and 1627 cm⁻¹ corresponding to O—H and H—O—H vibrations of Al₂O₃ are also observed. The bands of PW₁₁Cu between 900 and 500 cm⁻¹ are not visible due to overlapping with bands belonging to Al₂O₃. Slight shift in the bands along with absence of some bands in case of PW₁₁Cu/Al₂O₃ may be due to chemical interactions between PW₁₁Cu and the support.

Table 4 shows the FT-Raman frequencies of PW₁₁Cu and PW₁₁Cu/Al₂O₃ while the spectra are shown in figure S2. Characteristic bands at

**Fig. 5.** ³¹P MAS NMR of (a) PW₁₁Cu and (b) PW₁₁Cu/Al₂O₃.

996 cm⁻¹, 985 and 215 cm⁻¹, 967 and 946 cm⁻¹ corresponding to W=O symmetric stretch, W—O symmetric stretch and W—O—W symmetric stretch respectively are observed in case of PW₁₁Cu along with additional band at 483 cm⁻¹ corresponding to Cu—O symmetric stretch [22]. Similar bands are observed in case of PW₁₁Cu/Al₂O₃ indicating that the Keggin unit remains intact even after supporting. A slight shift in case of supported material indicates the successful supporting of PW₁₁Cu on to Al₂O₃ via chemical interactions.

Fig. 4 shows the H₂-TPR spectra of PW₁₁Cu and PW₁₁Cu/Al₂O₃. PW₁₁Cu shows maxima at 592 °C and 819 °C corresponding to formation of WO₃ species after decomposition of anion which is as expected [23]. However, the decrease in reduction temperature compared to reported ones is attributed to presence of Cs counter-cation, which leads to increase in consumption of H₂ gas [24].

The H₂-TPR curve of PW₁₁Cu/Al₂O₃ shows two maxima at 522 °C and 750 °C corresponding to PW₁₁Cu. Along with this, broad peaks are observed at temperatures above 800 °C analogous to the reduction of alumina. The decrease in the intensity as well as reduction temperatures of PW₁₁Cu in the supported material is attributed to strong chemical interactions between the active species and the support [25].

³¹P MAS NMR studies were carried out to understand the changes in the environment around phosphorus after supporting and also the interactions of the POM with support. PW₁₁Cu/Al₂O₃ shows a single peak at 6.01 ppm, which is downfield compared to unsupported PW₁₁Cu (-11.82 ppm) (Fig. 5). This downfield shift is attributed to two reasons. Firstly, some water molecules of PW₁₁Cu are lost when they are immobilized on to the support during impregnation [26]. Secondly, the existence of strong chemical interactions between PW₁₁Cu and Al₂O₃, as indicated in previous studies. The acidity of the medium caused by the POM results in the dehydroxylation of surface —O—H groups of alumina to give rise to electron donor and acceptor sites. These interact with the protons of the water molecules of PW₁₁Cu, thereby resulting in an overall negative charge over the Keggin unit. The negatively charged Keggin anions bind with the protonated support via electrostatic

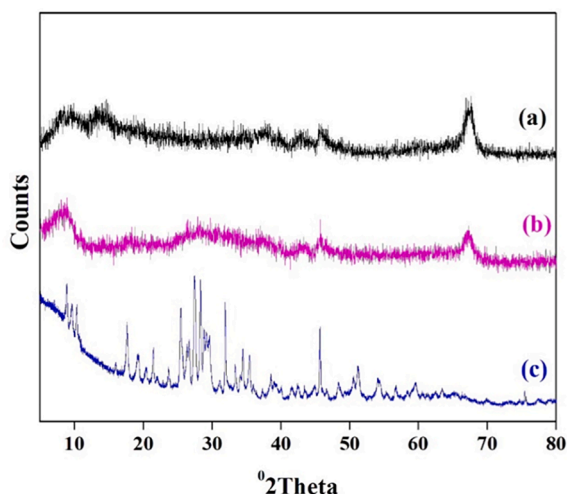


Fig. 6. Powder XRD of (a) Al_2O_3 , (b) $\text{PW}_{11}\text{Cu}/\text{Al}_2\text{O}_3$ and (c) PW_{11}Cu .

Table 5

BET Surface area of Al_2O_3 (support) and $\text{PW}_{11}\text{Cu}/\text{Al}_2\text{O}_3$ (supported catalyst).

Material	Surface area (m^2/g)	Pore diameter (\AA)
Al_2O_3	83	105
$\text{PW}_{11}\text{Cu}/\text{Al}_2\text{O}_3$	59	88

interactions and form strong chemical bonds also ensuring that PW_{11}Cu does not leach out from the support [27]. Similar type of interactions are also observed in case of other supports like SiO_2 and ZrO_2 [1,22,28].

Fig. 6 shows the wide angle powder XRD patterns of alumina, $\text{PW}_{11}\text{Cu}/\text{Al}_2\text{O}_3$ and PW_{11}Cu . Alumina shows reflection peaks at 37° , 48° and 66° 2θ corresponding to 311, 400 and 440 reflection planes and are in good agreement with reported work [27]. Powder XRD patterns of PW_{11}Cu show sharp crystalline peaks between 20° - 30° 2θ which are characteristic of Keggin unit, with a slight shift due to presence of copper [16]. In case of $\text{PW}_{11}\text{Cu}/\text{Al}_2\text{O}_3$, the sharp peaks disappear indicating homogeneous dispersion of PW_{11}Cu over the support.

BET surface area of Al_2O_3 and $\text{PW}_{11}\text{Cu}/\text{Al}_2\text{O}_3$ are shown in table 5 and the isotherms are shown in fig. 7. There is decrease in surface area of the supported material because of incorporation of PW_{11}Cu on to the support which is in agreement with the reported results [3]. This is

attributed to the fact that oxide supported catalysts tend to show decrease because of strong chemical interactions between the support and active species [29]. From the pore size distribution curve, the average pore diameter of the supported material was found to be 88 \AA .

3.2. Catalytic evaluation

The synthesized material was evaluated for its catalytic activity for the oxidation of styrene using *tert*-butyl hydroperoxide (TBHP) as oxidant. Initial experiments without catalyst and also using H_2O_2 (3 mL; Mole ratio of styrene: H_2O_2 – 10:30) as oxidant yielded negligible results, indicating that catalyst is essential for the reaction and that H_2O_2 would not suffice as oxidant for the reaction. Various reaction parameters like catalyst amount, reaction time, amount of TBHP and temperature were optimized for best possible conversion and selectivity of desired product (Fig. 8). Benzaldehyde and styrene-oxide were obtained as major products, while small quantities of acetophenone (selectivity ~ 8–10%) and benzoic acid (selectivity ~ 2–3%) were also obtained (Scheme 1).

The effect of catalyst amount was first studied keeping other parameters constant (Time – 16 h; temp – 60°C ; TBHP – 2 mL). On increase of catalyst amount from 10 mg to 25 mg, there is a steady increase in the conversion as well as selectivity of benzaldehyde, with a decrease in selectivity of styrene-oxide. This is expected because overall acidity of the system will increase with increase in catalyst amount. On further increase of catalyst amount, there is a decrease in the conversion and this may be explained as follows. At constant rate of agitation (700 rpm), increase in catalyst amount results in clumping of catalyst and as a result, blocking of catalytic sites occurs. Hence, 25 mg was considered optimum amount for the reaction.

Next, the reaction time was varied keeping other parameters constant (Catalyst amount – 25 mg; temp – 60°C ; TBHP – 2 mL). With increase in time from 4 h to 16 h, conversion increases. However, initially the selectivity of benzaldehyde decreases with increase in styrene-oxide selectivity and then both become constant. This may be explained as follows. It is well-known that styrene-oxide is the intermediate formed during the synthesis of benzaldehyde. In the present case, initially the selectivity for benzaldehyde is high. But as the reaction proceeds, an equilibrium is created between the intermediate and the final product, and hence the selectivity for benzaldehyde and styrene-oxide remain constant for the rest of the reaction. Beyond 16 h, there is negligible increase in the conversion and hence 16 h was considered optimum.

In order to optimize amount of oxidant, the reaction was carried out by adding different quantities of TBHP (catalyst amount – 25 mg; temp –

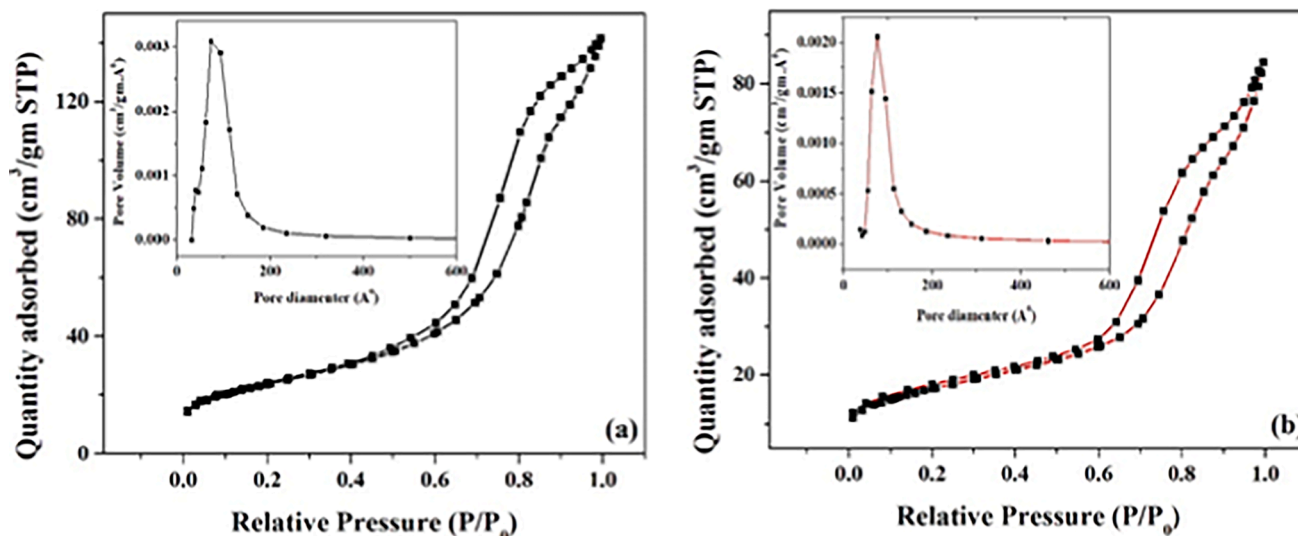


Fig. 7. N_2 sorption curves and (inset) average pore diameters of (a) Al_2O_3 and (b) $\text{PW}_{11}\text{Cu}/\text{Al}_2\text{O}_3$.

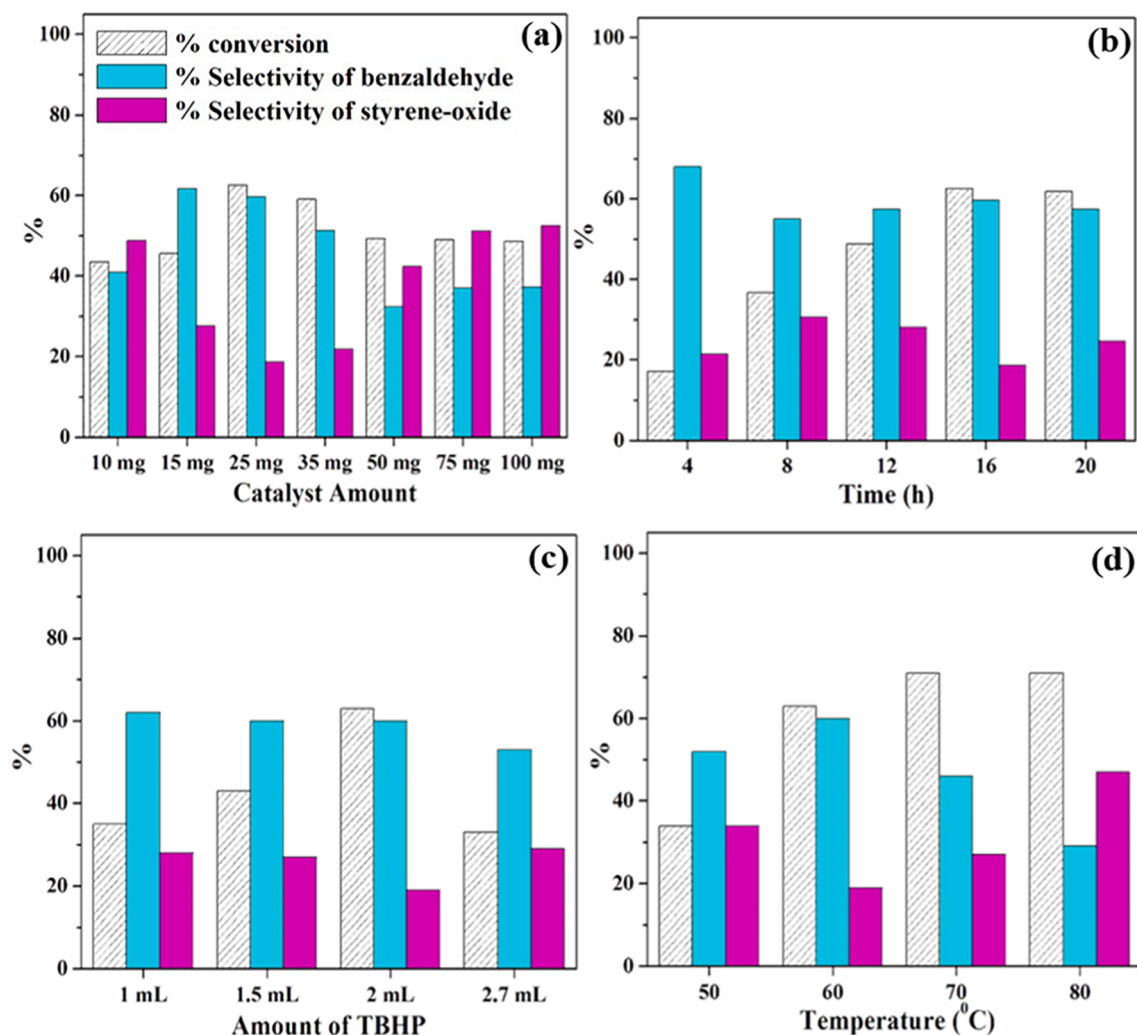
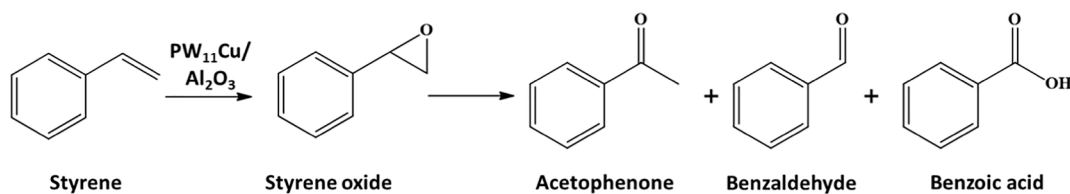


Fig. 8. Optimization of parameters for oxidation of styrene (a) Effect of catalyst amount (Time – 16 h; temp – 60 °C; TBHP – 2 mL; styrene-1 mL); (b) Effect of time (Catalyst amount – 25 mg; temp – 60 °C; TBHP – 2 mL; styrene-1 mL); (c) Effect of amount of TBHP (catalyst amount – 25 mg; temp – 60 °C; time – 16 h; styrene-1 mL); (d) Effect of temperature (catalyst amount – 25 mg; time – 16 h; TBHP – 2 mL; styrene-1 mL).



Scheme 1. Oxidation of styrene.

60 °C; time – 16 h). With increase in TBHP amount from 1 mL to 2 mL, there is a steady increase in conversion of styrene while the selectivity for benzaldehyde remains more or less constant. On further increase in TBHP amount to 2.7 mL, there is a drastic decrease in conversion as well as selectivity of desired products. This is because excess of TBHP results in higher concentration of oxygen which is used up in the oxidation of benzaldehyde to benzoic acid. Hence, 2 mL TBHP was considered optimum for the reaction. Varying results under varying amounts of TBHP also indicates that reaction rate depends on concentration of the oxidant.

Finally, the reaction was carried at different temperatures (catalyst amount – 25 mg; time – 16 h; TBHP – 2 mL) and the results are presented in fig. 8d. When the temperature was increased from 50 °C to 60 °C, there is an increase in conversion as well as selectivity of benzaldehyde.

But on increasing the temperature beyond 60 °C, there is a significant decrease in the selectivity due to the degradation of TBHP at higher temperatures, thereby resulting in polymerization of styrene. Hence, temperature was optimized at 60 °C.

3.3. Test for leaching and heterogeneity

The reaction mixture was subjected to treatment with 10% ascorbic acid solution at 60 °C after the completion of the reaction and separation of catalyst. Absence of blue color confirmed that $PW_{11}Cu$ does not leach out from the support.

To confirm the heterogeneous nature of the catalyst, the reaction was run for 12 h, after which, the catalyst was filtered out. Then the reaction was allowed to continue for further 4 h. No change was observed in the

Table 6

Heterogeneity test.

Reaction time	% conversion	% selectivity Styrene-oxide	Benzaldehyde
12 h	49	28	58
16 h	49	28	59

Catalyst amount: 25 mg; Time: 16 h; Temp: 60 °C; TBHP: 2 mL; Styrene-1 mL

Table 7

Role of support.

Catalyst	% conversion	% selectivity Styrene-oxide	Benzaldehyde	Turn Over Number (TON)
Al ₂ O ₃ ^[a]	NA	NA	NA	NA
PW ₁₁ Cu ^[b]	21	20	67	1102
PW ₁₁ Cu/ Al ₂ O ₃ ^[c]	63	19	60	3306
PW ₁₁ Cu/ ZrO ₂ ^[c] [22]	44	44	37	2309

^[a] Catalyst amount- 19.75 mg; TBHP – 2 mL; Temperature – 60 °C; Time-16 h; Styrene-1 mL.^[b] Catalyst amount- 6.25 mg; TBHP – 2 mL; Temperature – 60 °C; Time-16 h; Styrene-1 mL.^[c] Catalyst amount-25 mg (active amount of PW₁₁Cu – 6.25 mg); TBHP – 2 mL; Temperature – 60 °C; Time-16 h; Styrene-1 mL.

conversion as well as selectivity of the products, indicating that the catalyst is truly heterogeneous in nature Table 6.

3.4. Role of support

In order to understand the role of support, the reaction was carried out using the active amount of PW₁₁Cu present in the catalyst under optimized conditions, and the results are presented in table 7. It can be seen that the supported catalyst gives three times the conversion as that of unsupported one. This is attributed to two reasons: higher acidity of supported catalyst and homogeneous dispersion of active species on the support, due to which more number of active species are available for the reaction. Further, a comparison of the catalytic activity with that of PW₁₁Cu/ZrO₂ [22] shows that alumina is better support than zirconia, which may be due to the nature of support. Alumina contains Lewis acidic sites in the form of aluminium. The less nucleophilic intermediate formed, is able to desorb faster from PW₁₁Cu/Al₂O₃ as compared to PW₁₁Cu/ZrO₂, and hence gives higher conversion as well as higher selectivity for benzaldehyde, the complete oxidation product. This is further supported by thermodynamic studies.

3.5. Kinetics

Reaction kinetics plays an important role to help understand the role of each component of the reaction. In the present case, various experiments were carried out to obtain the rate and determine the order of reaction, and also the activation energy of the reaction.

It has already been determined that the reaction rate depends on concentration of both, styrene and TBHP (Fig. 8c and subsequent explanation). Further confirmation of the same can be obtained by carrying out the experiments under two different conditions.

First, when same concentration of styrene and TBHP is taken, a relation between the concentration and time can be established by Eq. (1), where 'a' is the initial concentrations of styrene and TBHP and 'x' is the conversion of styrene at time t

$$\frac{1}{(a-x)} = kt + c \quad (1)$$

Similarly, when different concentrations of substrate and TBHP are

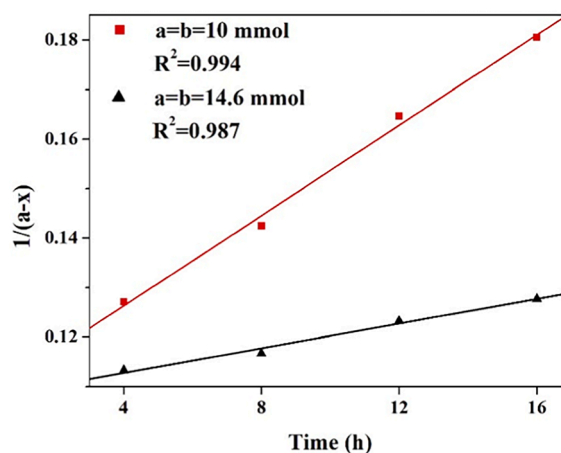


Fig. 9. Plot of 1/(a-x) versus time.

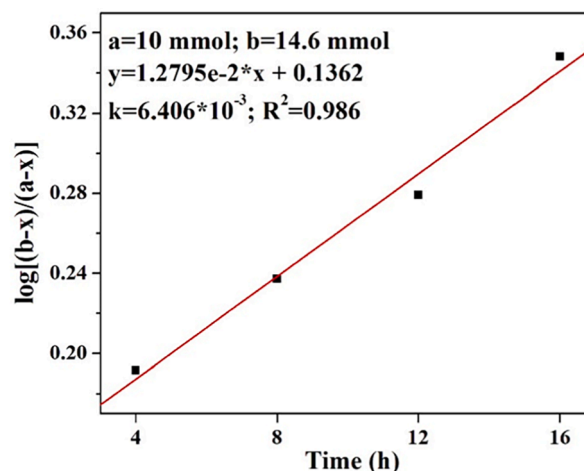


Fig. 10. Plot of log[(b-x)/(a-x)] versus time.

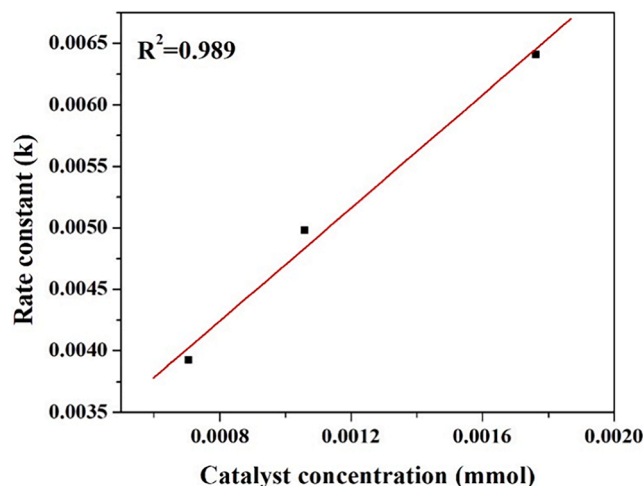


Fig. 11. Plot of rate of reaction versus catalyst concentration.

taken, a relation between individual concentrations and time is established by Eq. (2), where 'a' is the initial concentration of styrene, 'b' is the initial concentration of TBHP and 'x' is the concentration at time t.

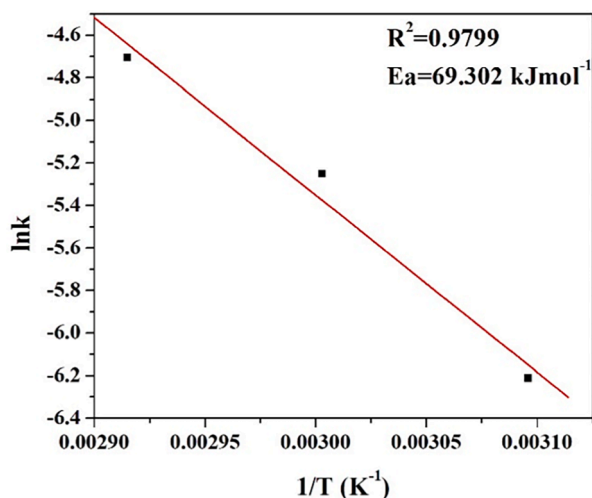


Fig. 12. Plot for determination of activation energy.

Table 8

Kinetic and thermodynamic parameters of styrene oxidation over $PW_{11}Cu/Al_2O_3$ as well as $PW_{11}Cu/ZrO_2$.

Catalyst	Activation energy (Ea, $kJmol^{-1}$)	Enthalpy (ΔH , $kJmol^{-1}$)	Entropy (ΔS , JK^{-1})	Gibbs' free energy (ΔG , J)
$PW_{11}Cu/Al_2O_3$	69.3	76.8	37.5	64,313
$PW_{11}Cu/ZrO_2$	40.3 [22]	31.1	-104	65,717

$$\frac{2.303}{(b-a)} \log \frac{a(b-x)}{b(a-x)} = kt \quad (2)$$

From Eq. (1), a plot of $1/(a-x)$ versus time (Fig. 9) shows a linear relationship indicating that the reaction follows second order kinetics with respect to concentration of styrene and TBHP overall.

Similarly, from Eq. (2), a plot of $\log[(b-x)/(a-x)]$ versus time (Fig. 10) gave a straight line indicating that, the reaction follows first order kinetics with respect to styrene and TBHP, individually [30].

The effect of rate of reaction with respect to concentration of catalyst was studied by carrying out the reaction at different catalyst concentrations. A plot of catalyst concentration versus rate constant gave a straight line, thereby indicating that the reaction follows first order with respect to catalyst concentration as well Fig. 11.

Finally, the effect of reaction temperature was studied as most oxidation reactions show very high sensitivity to temperature. A gradual increase in conversion of styrene is seen with increase in temperature from 333 K to 353 K and a plot of $1/T$ versus $\ln k$ shows linearity (Fig. 12). Based on this, the activation energy of the reaction was obtained using Arrhenius equation

$$k = Ae^{-E_a/RT}$$

In a two phase reaction system like the present one, it is necessary to know that the reaction is governed by a truly chemical step and is not diffusion/mass transfer limited. Generally, the E_a of a mass transfer limited reaction is known to be about 10–15 kJ/mol, while a truly chemical reaction has E_a value greater than 25 kJ/mol [31]. Significantly higher activation energy of 69.3 kJ/mol indicates that the reaction is truly governed by a chemical step and also that the catalyst has been exploited to its maximum capacity.

3.6. Thermodynamic studies

Thermodynamic parameters were calculated using the Eyring-

Table 9

Inhibition experiment using radical scavenger.

Reaction	Condition	% conversion	% selectivity	
			Styrene-oxide	Benzaldehyde
Styrene Oxidation	12 h	49	28	58
	16 h (after addition)	50	27	60

Catalyst amount: 25 mg; Temp: 60 °C; TBHP: 2 mL; Styrene-1 mL

Table 10

Regeneration study.

Catalyst	% Conversion	% Selectivity Benzaldehyde	Styrene-oxide
$PW_{11}Cu/Al_2O_3$	63	60	19
Rec ₁ - $PW_{11}Cu/Al_2O_3$	63	60	20
Rec ₂ - $PW_{11}Cu/Al_2O_3$	62	60	20
Rec ₃ - $PW_{11}Cu/Al_2O_3$	61	61	20

Catalyst amount – 25 mg; Time – 16 h; Temperature – 60 °C; TBHP – 2 mL; Styrene-1 mL

Polanyi equation given by eq. (4). A plot of $\ln(k/T)$ versus $1/T$ showed linearity and the enthalpy, ΔH , was calculated from the slope while the entropy, ΔS , was calculated from the intercept. These were further used to calculate the Gibbs' free energy using Eq. (5).

$$k = \frac{\kappa T}{h} e^{\frac{\Delta S}{R}} \cdot e^{-\frac{\Delta H}{RT}} \quad (4)$$

$$\Delta G = \Delta H - T\Delta S \quad (5)$$

The positive value for Gibbs' free energy confirms that the reaction is non-spontaneous. The values of ΔH , ΔS and ΔG are shown in table 8.

Table 8 shows a comparison of kinetic as well as thermodynamic parameters of styrene oxidation over $PW_{11}Cu/Al_2O_3$ as well as $PW_{11}Cu/ZrO_2$. Despite significantly higher activation energy and lower acidity (as mentioned in previous sections) compared to $PW_{11}Cu/ZrO_2$, $PW_{11}Cu/Al_2O_3$ shows higher conversion and higher selectivity for benzaldehyde. This is attributed to the positive entropy, which indicates greater favorability of the reaction. Positive entropy along with lower Gibbs' free energy illustrates that alumina as a support is more superior compared to zirconia for the present system.

3.7. Inhibition experiment using radical scavenger

It is well known that transition metal catalyzed oxidation reactions follow either peroxy-intermediate formation or proceed via radical mechanism [7]. In order to gain an idea on the same, a radical scavenger approach was used. 2, 6-di-tertbutyl-4-methyl phenol was used as a radical scavenger and was added into the system after 12 h of the reaction. The results presented in table 9 showed that there was no significant increase in conversion as well as selectivity of epoxide, indicating that the reaction followed radical mechanism as expected [22].

3.8. Regeneration study

Regeneration of the catalyst was carried out by simple centrifugation method followed by washing with methanol and drying. The regenerated catalyst was evaluated for its activity for the same reaction under optimized conditions and the results are presented in Table 10. No changes in the conversion as well as selectivity of products even after three cycles indicate that the catalyst can be reused multiple times.

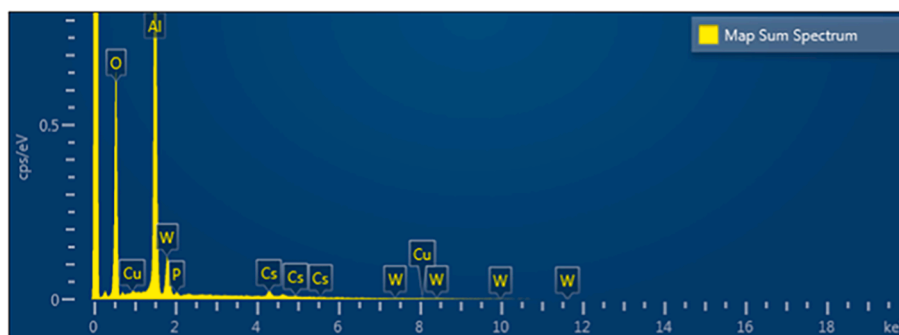


Fig. 13. EDX of EDX values of Regenerated $PW_{11}Cu/Al_2O_3$.

Table 11

FT-IR frequencies of fresh and regenerated $PW_{11}Cu/Al_2O_3$.

FT-IR Frequencies (cm^{-1})	P—O	W=O	W—O—W	Cu—O	O—H	H—O—H	O—H—O
$PW_{11}Cu/Al_2O_3$	1099 1064	—	—	—	3437	1627	—
Rec. $PW_{11}Cu/Al_2O_3$	1101 1067	—	—	—	3443	1604	—

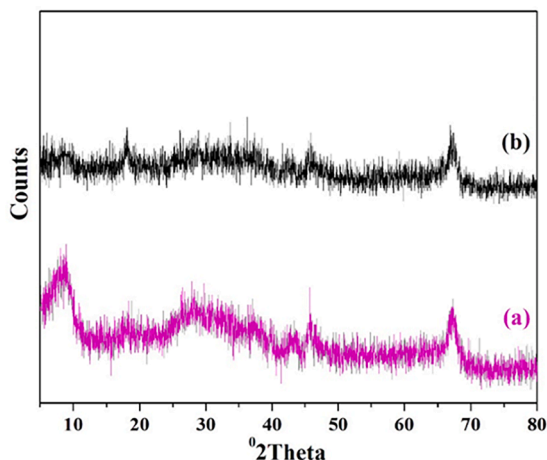


Fig. 14. Powder XRD of (a) Fresh and (b) recycled $PW_{11}Cu/ZrO_2$.

3.9. Characterization of regenerated catalyst

The regenerated catalyst was characterized by EDX, FT-IR as well as powder XRD. EDX values of Regenerated $PW_{11}Cu/Al_2O_3$ value (% wt): P, 0.21; W, 13.96; Cu, 0.39; Cs; 4.64 are in good agreement with that of fresh catalyst, indicating no leaching of Cu during the reaction (Fig. 13).

Regenerated $PW_{11}Cu/Al_2O_3$ shows Table 11 the same FT-IR bands as that of the fresh one, indicating that the structural morphology of the catalyst remains intact even after the completion of the reaction.

Powder XRD of fresh and recycled $PW_{11}Cu/Al_2O_3$ is shown in Fig. 14. The dispersed spectra is retained in case of recycled catalyst indicating that the catalyst remains dispersed during the course of the reaction and also after recycling.

4. Conclusion

Intact structure of $PW_{11}Cu$ after supporting on alumina was confirmed by IR and Raman, while uniform dispersion was confirmed by XRD and TPR, and NMR studies established the chemical interactions between support and active species. Despite its neutral nature, alumina increased the activity of $PW_{11}Cu$, clearly observed in its catalytic

evaluation, which showed higher conversion and higher selectivity for benzaldehyde compared to zirconia supported $PW_{11}Cu$, which is more acidic in nature. This behaviour was attributed to presence of Lewis acidic sites in the form of aluminum, and was further established by thermodynamic studies, which gave positive entropy along with lower Gibbs' free energy compared to zirconia supported one.

Author contributions

The manuscript was written through contributions of all authors. All authors have given approval to the final version of the manuscript.

CRediT authorship contribution statement

Rajesh Sadasivan: Conceptualization, Methodology, Writing - review & editing, Supervision. **Anjali Patel:** Visualization, Investigation, Data curation, Validation, Writing - original draft.

Declaration of Competing Interest

The authors declare that they have no known competing financial interests or personal relationships that could have appeared to influence the work reported in this paper.

Acknowledgments

The authors would like to acknowledge Department of Science and Technology (DST), Govt. of India, Project No. SR/S1/IC-36/2012 for financial support. Sincere thanks to Department of Chemistry, The Maharaja Sayajirao University of Baroda for BET, Department of Physics, The Maharaja Sayajirao University of Baroda for FT-Raman analyses and Department of Geology, The Maharaja Sayajirao University of Baroda for EDX analysis. We also acknowledge Prof. N. Lingaiah, CSIR-IICT, Hyderabad, for H_2 -TPR studies. One of the authors, RS is thankful to Council of Scientific and Industrial Research (CSIR), Govt. of India, for award of Senior Research Fellowship (SRF).

Appendix A. Supplementary data

Supplementary data to this article can be found online at <https://doi.org/10.1016/j.ica.2021.120357>.

References

- [1] J. Alcañiz-Monge, B.E. Bakkali, G. Trautwein, S. Reinoso, Zirconia-supported tungstophosphoric heteropolyacid as heterogeneous acid catalyst for biodiesel production, *Appl. Catal. B: Environ.* 224 (2018) 194–203.
- [2] R. Hajian, F. Jafari, Zinc polyoxometalate immobilized on ionic liquid-modified MCM-41: an efficient reusable catalyst for the selective oxidation of alcohols with hydrogen peroxide, *J. Iranian Chem. Soc.* 16 (3) (2019) 563–570.
- [3] L. Hong, P. Win, X. Zhang, W. Chen, H.N. Miras, Y.-F. Song, Covalent immobilization of polyoxotungstate on alumina and its catalytic generation of sulfoxides, *Chem. Eur. J.* 22 (2016) 11232–11238.
- [4] A.M. Hussein, A.H. Mady, S. Mahmoud, J.J. Shim, F.Z. Yehia, Synthesis of polyoxometalates supported on HZSM-5 for the photocatalytic purification of crude terephthalic acid under mild conditions, *J. Photochem. Photobiol., A: Chem.* 377 (2019) 173–181.
- [5] R.A. Frenzel, G.P. Romanelli, M.N. Blanco, L.R. Pizzio, Transition metal-modified polyoxometalates supported on carbon as catalyst in 2-(methylthio)-benzothiazole sulfoxidation, *J. Chem. Sci.* 127 (2015) 123–132.
- [6] A. Patel, S. Singh, Novel dilacunary phosphotungstate supported onto zirconia: synthesis, characterization and versatile catalytic activity, *J. Taiwan Inst. Chem. Eng.* 64 (2016) 306–313.
- [7] S. Singh, A. Patel, Environmentally benign oxidations of alkenes and alcohols to corresponding aldehydes over anchored phosphotungstates: effect of supports as well as oxidants, *Catal. Lett.* 146 (6) (2016) 1059–1072.
- [8] N. Narkhede, A. Patel, S. Singh, Mono lacunary phosphomolybdate supported on MCM-41: synthesis, characterization and solvent free aerobic oxidation of alkenes and alcohols, *Dalton Trans.* 43 (6) (2014) 2512–2520.
- [9] S. Pathan, A. Patel, Selective green oxidation of alcohols and alkenes with molecular oxygen using supported undecamolybdophosphate under solvent free condition, *Chem. Eng. J.* 243 (2014) 183–191.
- [10] A. Patel, S. Pathan, Solvent free selective oxidation of styrene and benzyl alcohol to benzaldehyde over an eco-friendly and reusable catalyst, undecamolybdophosphate supported onto neutral alumina, *Ind. Eng. Chem. Res.* 51 (2) (2012) 732–740.
- [11] J. Hu, K. Li, W. Li, F. Ma, Y. Guo, Selective oxidation of styrene to benzaldehyde catalyzed by Schiff base-modified ordered mesoporous silica materials impregnated with the transition metal-monosubstituted Keggin-type polyoxometalates, *Appl. Catal. A: Gen.* 364 (1–2) (2009) 211–220.
- [12] L.S. Nogueira, S. Ribeiro, C.M. Granadeiro, E. Pereira, G. Feio, L. Cunha-Silva, S. S. Balula, Novel polyoxometalate silica nano-sized spheres: efficient catalysts for olefin oxidation and the deep desulfurization process, *Dalton Trans.* 43 (25) (2014) 9518–9528.
- [13] A. Patel, S. Pathan, P. Prakashan, One pot oxidative esterification of benzaldehyde over a supported Cs-salt of mono nickel substituted phosphotungstate, *RSC Adv.* 6 (56) (2016) 51394–51402.
- [14] VY Evtushok, OY Podyacheva, AN Suboch, NV Maksimchuk, OA Stonkus, LS Kibis, OA Kholdeeva, H₂O₂-based selective oxidations by divanadium-substituted polyoxotungstate supported on nitrogen-doped carbon nanomaterials, *Catal. Today.* 354 (2020) 196–203.
- [15] J. North, O. Poole, A. Alotaibi, H. Bayahia, E.F. Kozhevnikova, A. Alsalmeh, M.R. H. Siddiqui, I.V. Kozhevnikov, Efficient hydrodesulfurization catalysts based on Keggin polyoxometalates, *Appl. Catal. A: Gen.* 508 (2015) 16–24.
- [16] A.U. Patel, R. Sadasivan, Cs Salt of Undecatungstophospho(aqua) Cuprate(II): microwave synthesis, characterization, catalytic and kinetic study for epoxidation of cis-cyclooctene with TBHP, *ChemistrySelect* 3 (39) (2018) 11087–11097.
- [17] H. Ranjan Sahu, G. Ranga Rao, Characterization of combustion synthesized zirconia powder by UV-vis, IR and other techniques, *Bull. Mater. Sci.* 23 (2000) 349–354.
- [18] P. Vázquez, L. Pizzio, C. Cáceres, M. Blanco, H. Thomas, E. Alesso, L. Finkielstein, B. Lantano, G. Moltrasio, J. Aguirre, Silica-supported heteropolyacids as catalysts in alcohol dehydration reactions, *J. Mol. Catal. A: Chem.* 161 (2000) 223–232.
- [19] S. Singh, A. Patel, 12-Tungstophosphoric acid supported on mesoporous molecular material: synthesis, characterization and performance in biodiesel production, *J. Cleaner Prod.* 72 (2014) 46–56.
- [20] K.M. Parida, A.C. Pradhan, J. Das, N. Sahu, Synthesis and characterization of nano-sized porous gamma-alumina by control precipitation method, *Mater. Chem. Phys.* 113 (2009) 244–248.
- [21] P. Colombari, Raman study of the formation of transition alumina single crystal from protonic β/β' aluminas, *J. Mater. Sci. Lett.* 7 (1988) 1324–1326.
- [22] R. Sadasivan, A. Patel, Flexible oxidation of styrene using TBHP over zirconia supported mono-copper substituted phosphotungstate, *RSC Adv.* 9 (48) (2019) 27755–27767.
- [23] J.A. Gamelas, F.A.S. Couto, M.C.N. Trovão, A.M.V. Cavaleiro, J.A.S. Cavaleiro, J.D. P. de Jesus, Investigation of the thermal decomposition of some metal-substituted Keggin tungstophosphates, *Thermochim. Acta* 326 (1999) 165–173.
- [24] S. Liu, L.u. Chen, G. Wang, J. Liu, Y. Gao, C. Li, H. Shan, Effects of Cs-substitution and partial reduction on catalytic performance of Keggin-type phosphomolybdic polyoxometalates for selective oxidation of isobutane, *J. Energy Chem.* 25 (1) (2016) 85–92.
- [25] M. Shimokawabe, H. Asakawa, N. Takezawa, Characterization of copper/zirconia catalysts prepared by an impregnation method, *Appl. Catal.* 59 (1990) 45–58.
- [26] S. Thanasilp, J.W. Schwank, V. Meeyoo, S. Pengpanich, M. Hunsom, Preparation of supported POM catalysts for liquid phase oxydehydrogenation of glycerol to acrylic acid, *J. Mol. Catal. A: Chem.* 380 (2013) 49–56.
- [27] A. Kurhade, A.K. Dalai, Physicochemical characterization and support interaction of alumina-supported heteropolyacid catalyst for biodiesel production, *Asia-Pacific J. Chem. Eng.* 13 (6) (2018) e2249, <https://doi.org/10.1002/apj.2249>.
- [28] S. Singh, A. Patel, Selective solvent free oxidation of aldehydes to carboxylic acids over anchored 12-tungstophosphoric acid using different oxidants, *J. Taiwan Inst. Chem. Eng.* 52 (2015) 120–126.
- [29] A. Patel, A. Patel, Nickel exchanged supported 12-tungstophosphoric acid: synthesis, characterization and base free one-pot oxidative esterification of aldehyde and alcohol, *RSC Adv.* 9 (3) (2019) 1460–1471.
- [30] Y. Liang, C. Yi, S. Tricard, J. Fang, J. Zhao, W. Shen, Prussian blue analogues as heterogeneous catalysts for epoxidation of styrene, *RSC Adv.* 5 (23) (2015) 17993–17999.
- [31] G.C. Bond, *Heterogeneous Catalysis: Principles and Applications*, Clarendon Press, Oxford, 1974.